



Tuning Nanofiber Morphology and Hydrophobicity via PVDF-co-HFP Polymer Concentration

Naufaldin Adam Na'im¹ Aditya Rianjanu^{1,2}  

¹Department of Materials Engineering, Faculty of Industrial Technology, Institut Teknologi Sumatera, Terusan Ryacudu, Way Hui, Jati Agung, Lampung Selatan, 35365 Indonesia

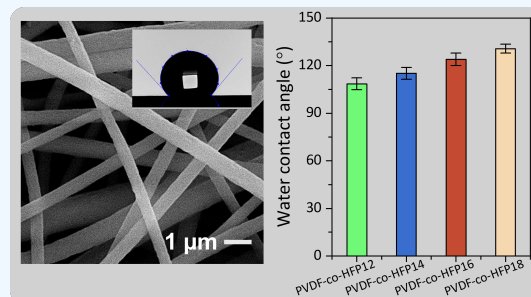
²Center for Green and Sustainable Materials, Institut Teknologi Sumatera, Terusan Ryacudu, Way Hui, Jati Agung, Lampung Selatan 35365, Indonesia

✉ **Corresponding author:** aditya.rianjanu@mt.itera.ac.id (AR)

 **ARTICLE HISTORY:**  Received: May 21, 2025 |  Revised: June 11, 2025 |  Accepted: June 16, 2025

ABSTRACT

This study investigates the effect of poly(vinylidene fluoride-co-hexafluoropropylene) (PVDF-co-HFP) concentration on the morphological and surface wettability properties of electrospun nanofibers. Nanofiber mats were fabricated using electrospinning with PVDF-co-HFP concentrations ranging from 12 wt% to 18 wt%. Scanning electron microscopy (SEM) analysis revealed that increasing polymer concentration resulted in larger and more uniform fiber diameters, ranging from approximately 235 nm to 560 nm. Fourier-transform infrared (FTIR) spectroscopy confirmed the preservation of the chemical structure, with characteristic peaks associated with CF₂ and C–F groups, and the presence of both α - and β -phases of PVDF. Water contact angle (WCA) measurements indicated a marked increase in hydrophobicity, with WCA values rising from ~108° for PVDF-co-HFP12 to ~128° for PVDF-co-HFP18. This enhancement is attributed to increased surface roughness and fiber diameter, in line with the Cassie–Baxter wetting model. The results demonstrate that polymer concentration is a critical parameter in tailoring nanofiber morphology and wettability, providing a straightforward strategy for designing functional materials in applications such as water-repellent coatings, filtration membranes, and sensing platforms.



Keywords: PVDF-co-HFP, Electrospinning, Nanofiber, Water Contact Angle, surface Wettability

1. INTRODUCTION

Electrospinning has emerged as a versatile and scalable technique for fabricating nanofiber membranes with applications in filtration, sensors, biomedical scaffolds, and surface coatings [1, 2]. Among the various polymers employed, poly(vinylidene fluoride-co-hexafluoropropylene) (PVDF-co-HFP) stands out due to its excellent chemical resistance, thermal stability, mechanical flexibility, and intrinsic hydrophobicity, making it ideal for advanced functional materials [3, 4]. The performance of electrospun nanofibers is closely linked to their morphological and surface properties, which are, in turn, governed by processing parameters such as polymer concentration, solution viscosity, and electrospinning conditions [5, 6, 7]. Among these, polymer concentration plays a pivotal role in determining fiber diameter, uniformity, and surface roughness, parameters that significantly influence wettability, permeability, and mechanical behavior [8, 9]. Despite numerous studies on PVDF-based nanofibers, detailed insights into the relationship between PVDF-co-HFP concentration and both fiber morphology and surface wetting characteristics remain limited.

Understanding this correlation is critical, especially for applications where surface wettability dictates performance, such as in water-repellent membranes and biointerface engineering [10, 11, 12]. Water contact angle (WCA) is a reliable

measure of surface hydrophobicity and serves as a direct indicator of how nanostructure geometry affects wetting behavior. In this context, controlling fiber diameter through polymer concentration can provide a tunable method for tailoring surface functionality. This study aims to systematically investigate the influence of PVDF-co-HFP concentration on the morphological and wettability properties of electrospun nanofibers. We focus on analyzing the fiber diameter using SEM, verifying chemical structure via FTIR spectroscopy, and evaluating surface hydrophobicity through static WCA measurements. The findings offer a deeper understanding of how microstructural control via polymer concentration can be leveraged to engineer nanofibers with desired surface properties for specific applications.

Although various studies have reported on the electrospinning of PVDF-based polymers [13, 14], most have addressed general processing effects or focused on blended systems, with limited emphasis on systematically isolating the role of PVDF-co-HFP concentration. To date, there remains a lack of comprehensive investigations that directly correlate polymer concentration with both nanofiber morphology and wettability behavior. Addressing this gap, the present study systematically examines how varying PVDF-co-HFP concentrations affect fiber diameter, structural characteristics, and surface hydrophobicity. By linking concentration-dependent morphological features to wettability outcomes, this work

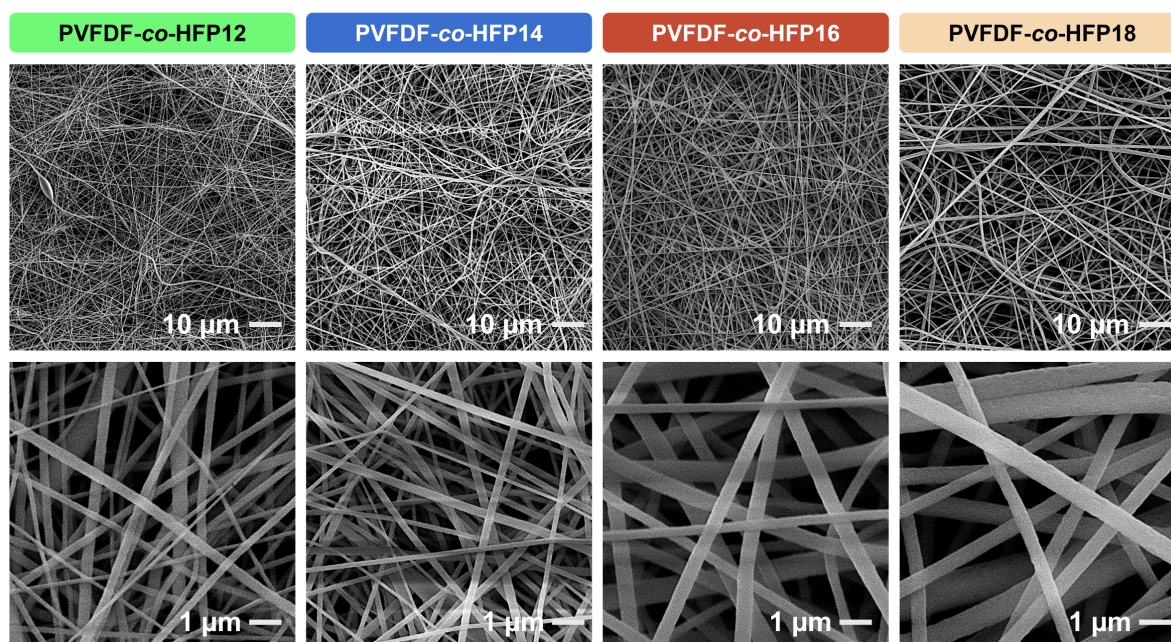


Figure 1. Scanning electron microscopy (SEM) images of electrospun PVDF-co-HFP nanofibers prepared at different polymer concentrations: 12 wt%, 14 wt%, 16 wt%, and 18 wt%.

provides new insights into microstructural control strategies for engineering nanofiber surfaces with tunable hydrophobic properties, offering practical relevance for applications such as water-repellent membranes, coatings, and biomedical scaffolds.

2. MATERIALS AND METHODS

2.1 Materials

Poly(vinylidene fluoride-co-hexafluoropropylene) (PVDF-co-HFP) with an average molecular weight (Mw) of ~400,000 and number average molecular weight (Mn) of ~130,000 in pellet form was obtained from Sigma-Aldrich. Dimethylformamide (DMF) and acetone, both of analytical grade, were purchased from Merck and used as received.

2.2 Preparation of PVDF-co-HFP nanofiber

Solutions of PVDF-co-HFP were prepared at concentrations of 12 wt%, 14 wt%, 16 wt%, and 18 wt% by dissolving the polymer in a 6:4 (v/v) mixture of DMF and acetone to a total volume of 10 mL. The mixtures were magnetically stirred at 60°C and 600 rpm until complete dissolution of the polymer was achieved. Electrospinning was performed using a high-voltage power supply with an applied voltage of 10 kV, a tip-to-collector distance of 15 cm, and a flow rate of 1 mL/h. The electrospinning process was maintained for 8 hours to ensure adequate nanofiber mat formation. The electrospinning process was conducted at ambient conditions, with a recorded temperature of approximately $25 \pm 2^\circ\text{C}$ and relative humidity of $60 \pm 5\%$.

2.3 Materials characterizations

The surface morphology and fiber diameter of the electrospun nanofibers were characterized using scanning electron microscopy (SEM, JEOL JSM-6510). Chemical bonding and functional groups were analyzed via Fourier-transform infrared spectroscopy (FTIR) using a Shimadzu IRSpirit-X Com-

pact FTIR Spectrometer. Water contact angle (WCA) measurements were carried out using a custom-built contact angle measurement setup to evaluate the wettability of the nanofiber surfaces.

3. RESULTS AND DISCUSSION

The morphological evolution of electrospun PVDF-co-HFP nanofibers with varying polymer concentrations (12–18 wt%) is shown in Figure 1, complemented by the corresponding fiber diameter measurements in Figure 2. At polymer concentration of 12 wt% (i.e., PVDF-co-HFP12), the SEM images reveal the formation of thin, randomly oriented nanofibers with slightly non-uniform diameters and minor bead presence, which is indicative of insufficient solution viscosity and poor chain entanglement during electrospinning process [15]. This is quantitatively confirmed by the average fiber diameter of approximately 245 nm (Figure 2a). As the polymer concentration increases to 14 wt% (i.e., PVDF-co-HFP14), the nanofiber morphology becomes more homogeneous, with smoother and thicker fibers. The mean diameter rises to approximately 371 nm, suggesting improved jet stability due to enhanced viscosity and surface tension balance. At 16 wt% (PVDF-co-HFP16), a further increase in diameter to 475 nm is observed, accompanied by a more densely packed and uniform fiber network. At the highest tested concentration (18 wt%), the fibers exhibit the most uniform morphology and the largest average diameter of 590 nm. The high viscosity of this solution limits the stretching of the polymer jet, resulting in larger fiber diameters and highly aligned networks with minimal structural defects [16].

The Fourier-transform infrared (FTIR) spectrum of the electrospun PVDF-co-HFP nanofibers (Figure 2b) reveals the presence of characteristic vibrational modes confirming the chemical structure of the copolymer. Prominent absorption peaks are observed at 3021 and 2978 cm^{-1} , which correspond to the symmetric and asymmetric stretching vibrations

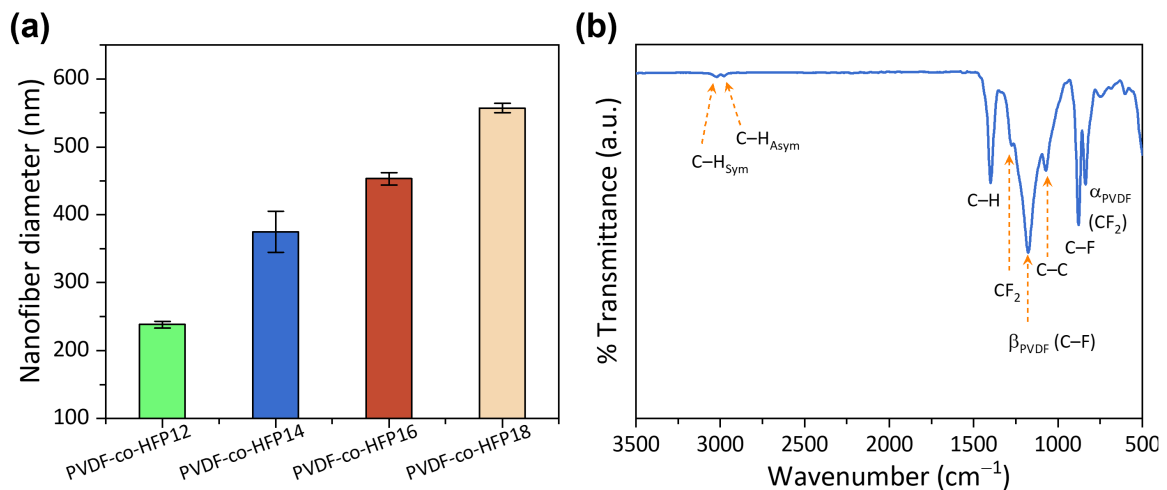


Figure 2. (a) Average nanofiber diameter of PVDF-co-HFP nanofibers as a function of polymer concentration, showing an increasing trend with higher concentrations. Error bars represent standard deviations. (b) FTIR spectrum of PVDF-co-HFP nanofibers, confirming characteristic vibrational bands associated with the polymer backbone.

of -CH bonds, respectively. These peaks are commonly attributed to the aliphatic hydrocarbon chains in the polymer backbone. A strong absorption band around 1398 cm^{-1} is associated with the bending vibrations of CH_2 groups, while the peak at 1275 cm^{-1} can be ascribed to CF_2 stretching. The band at 1176 cm^{-1} is indicative of β -phase PVDF, typically assigned to C-F stretching vibrations. This is a significant feature as the β -phase is known for its piezoelectric and ferroelectric properties, which can influence the functional behavior of the nanofibers. In addition, peaks at 1072 and 878 cm^{-1} are attributed to C-C and C-F stretching vibrations, respectively, further confirming the integrity of the PVDF-co-HFP structure. The absorption at 749 and 686 cm^{-1} corresponds to the CF_2 rocking mode, typically associated with the α -phase of PVDF. This indicates the presence of a semi-crystalline structure with both α - and β -phase contributions [17, 18]. Overall, the FTIR data confirms the successful retention of the copolymer's molecular structure during the electrospinning process. The coexistence of α - and β -phases suggests a partially crystalline morphology, which may influence the material's mechanical and surface properties, such as wettability and stiffness.

Figure 3 illustrates the surface wettability behavior of PVDF-co-HFP nanofiber mats, assessed via static water contact angle (WCA) measurements. Figure 3a presents representative side-view images of water droplets on nanofiber surfaces, while Figure 3b quantifies the corresponding contact angles. The sample PVDF-co-HFP12 (12 wt%) exhibits an average WCA of approximately 108° , indicative of a moderately hydrophobic surface. With increased polymer concentration, the WCA also increases: PVDF-co-HFP14 (14 wt%) reaches $\sim 115^\circ$, PVDF-co-HFP16 (16 wt%) shows $\sim 123^\circ$, and PVDF-co-HFP18 (18 wt%) achieves the highest angle at $\sim 30^\circ$ (Figure 3b) [19, 20, 21].

A strong positive correlation is observed between the diameter of electrospun PVDF-co-HFP nanofibers and their corresponding water contact angle (WCA), as demonstrated in Figures 2a and 3b. As the polymer concentration increases from 12 wt% (PVDF-co-HFP12) to 18 wt% (PVDF-co-HFP18), the average fiber diameter increases significantly—from ap-

proximately 235 nm to over 550 nm. This morphological evolution is directly accompanied by a progressive enhancement in surface hydrophobicity, with WCA values rising from $\sim 108^\circ$ to $\sim 128^\circ$. From a physicochemical standpoint, this trend can be explained by considering the effect of fiber diameter on surface roughness and porosity, which play pivotal roles in wetting behavior. In electrospun membranes, smaller-diameter fibers typically form densely packed, highly porous mats with high surface area-to-volume ratios [22, 23]. While this may enhance absorption or permeation in some applications, such fine structures often lead to incomplete air pocket formation beneath a water droplet, reducing the apparent hydrophobicity. As fiber diameter increases, the surface topography becomes coarser, and the inter-fiber spacing becomes more regular and well-defined. This enables a greater fraction of the droplet to rest on air pockets between fibers, minimizing solid-liquid contact area [24]. According to the Cassie-Baxter model, this condition leads to an increased apparent contact angle, as the droplet effectively sits on a composite surface of solid and air [25, 26]. Hence, larger nanofiber diameters contribute to enhanced surface roughness at the microscale, which amplifies the intrinsic hydrophobic nature of the PVDF-co-HFP polymer. Moreover, thicker fibers result from higher solution viscosity during electrospinning, which stabilizes the jet and reduces the incidence of bead formation. Beads, often present in low-viscosity solutions, create wettable defects on the surface, lowering the WCA. Therefore, the absence of such defects in higher-diameter fibers further contributes to the observed increase in hydrophobicity. This relationship between decreasing fiber diameter and increasing hydrophobicity is of practical significance for designing water-repellent materials, particularly in applications such as self-cleaning surfaces, protective coatings, and membrane technology.

4. CONCLUSION

In this study, we successfully fabricated PVDF-co-HFP nanofiber mats via electrospinning by varying polymer concentrations from 12 wt% to 18 wt%. The morphological analysis using SEM revealed that increasing the polymer concentration

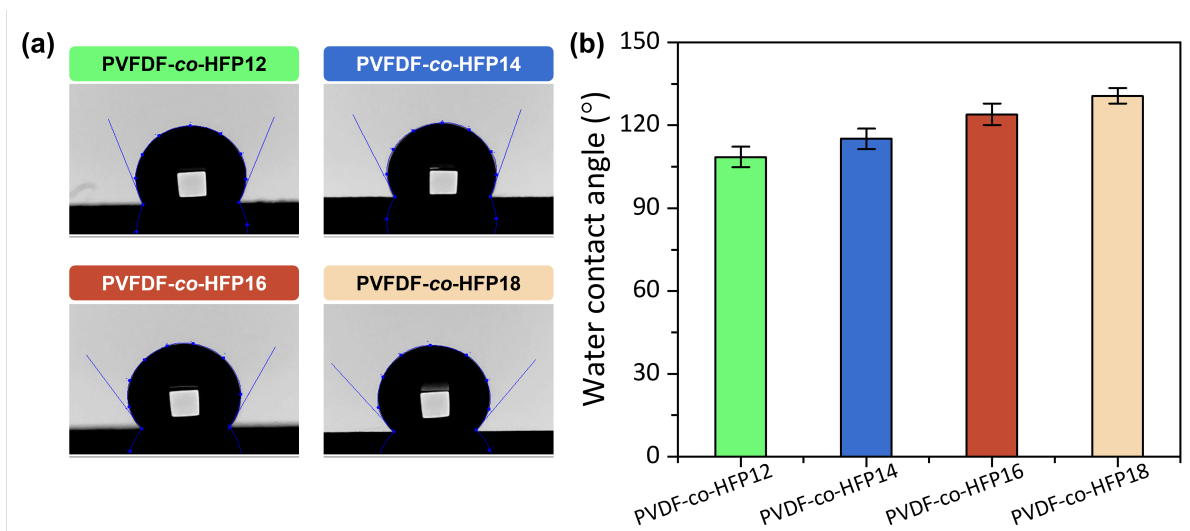


Figure 3. (a) Representative water contact angle (WCA) images of PVDF-co-HFP nanofiber mats fabricated with varying polymer concentrations. (b) Quantitative analysis of the WCA values, indicating an increase in surface hydrophobicity with higher PVDF-co-HFP concentrations. Error bars represent standard deviations based on multiple measurements.

led to a significant increase in nanofiber diameter, from approximately 235 nm (PVDF-co-HFP12) to 560 nm (PVDF-co-HFP18), with more uniform and bead-free structures observed at higher concentrations. FTIR spectroscopy confirmed the chemical integrity of the electrospun PVDF-co-HFP nanofibers, showing characteristic vibrational bands associated with CF_2 , C-F, C-C, and CH groups, with evidence of both α - and β -phases of PVDF. Water contact angle measurements demonstrated a consistent increase in hydrophobicity with fiber diameter, from $\sim 108^\circ$ for PVDF-co-HFP12 to $\sim 128^\circ$ for PVDF-co-HFP18. This enhancement is attributed to increased surface roughness and air entrapment in the nanofiber network, consistent with the Cassie-Baxter wetting model. Overall, this work highlights that PVDF-co-HFP concentration is a critical parameter in controlling nanofiber morphology and surface wettability. The ability to tune these properties through simple formulation adjustment offers a promising route for optimizing electrospun membranes for specific applications such as waterproof coatings, separation membranes, and functional sensor interfaces. Future studies will explore the effects of thermal or chemical post-treatment, as well as assess the long-term stability of hydrophobic performance under environmental stressors such as UV exposure and humidity fluctuations.

DATA AVAILABILITY STATEMENT

The datasets generated during and/or analyzed during the current study are available from the corresponding author on reasonable request.

CONFLICT OF INTEREST

The authors declare that there are no conflicts of interest.

REFERENCES

- [1] J. Xue, T. Wu, Y. Dai, Y. Xia, *Electrospinning and Electrospun Nanofibers: Methods, Materials, and Applications*, Chemical Reviews 119 (8) (2019) 5298–5415. <https://doi.org/10.1021/acs.chemrev.8b00593>.
- [2] A. M. Yessuf, M. Bahri, T. S. Kassa, B. P. Sharma, A. M. Salama, C. Xing, Q. Zhang, Y. Liu, *Electrospun Polymeric Nanofibers: Current Trends in Synthesis, Surface Modification, and Biomedical Applications*, ACS Applied Bio Materials 7 (7) (2024) 4231–4253. <https://doi.org/10.1021/acsabm.4c00307>.
- [3] D. Ponnamma, O. Aljarod, H. Parangusan, M. A. Ali Al-Maadeed, *Electrospun nanofibers of PVDF-HFP composites containing magnetic nickel ferrite for energy harvesting application*, Materials Chemistry and Physics 239 (2020) 122257. <https://doi.org/10.1016/j.matchemphys.2019.122257>.
- [4] Z. Chen, M. Guan, Y. Cheng, H. Li, G. Ji, H. Chen, X. Fu, D. E. Awuye, Y. Zhu, X. Yin, Z. Man, C. Wu, *Boehmite-enhanced poly(vinylidene fluoride-co-hexafluoropropylene)/polyacrylonitrile (PVDF-HFP/PAN) coaxial electrospun nanofiber hybrid membrane: a superior separator for lithium-ion batteries*, Advanced Composites and Hybrid Materials 6 (6) (2023) 219. <https://doi.org/10.1007/s42114-023-00794-2>.
- [5] Y. Zu, Z. Duan, Z. Yuan, Y. Jiang, H. Tai, *Electrospun nanofiber-based humidity sensors: materials, devices, and emerging applications*, Journal of Materials Chemistry A 12 (40) (2024) 27157–27179. <https://doi.org/10.1039/D4TA05042H>.
- [6] B. Subeshan, A. Atayo, E. Asmatulu, *Machine learning applications for electrospun nanofibers: a review*, Journal of Materials Science 59 (31) (2024) 14095–14140. <https://doi.org/10.1007/s10853-024-09994-7>.
- [7] M. Aman Mohammadi, S. Dakhili, A. Mirza Alizadeh, S. Kooki, H. Hassanzadazar, M. Alizadeh-Sani, D. J. McClements, *New perspectives on electrospun nanofiber applications in smart and active food packaging materials*, Critical Reviews in Food Science and Nutrition 64 (9) (2024) 2601–2617. <https://doi.org/10.1080/10408398.2022.2124506>.
- [8] U. Duru Kamaci, A. Peksel, *Enhanced Catalytic Activity of Immobilized Phytase into Polyvinyl Alcohol-Sodium Alginate Based Electrospun Nanofibers*, Catalysis Letters 151 (3) (2021) 821–831. <https://doi.org/10.1007/s10562-020-03339-0>.
- [9] V. Beachley, X. Wen, *Effect of electrospinning parameters on the nanofiber diameter and length*, Materials Science and Engineering: C 29 (3) (2009) 663–668. <https://doi.org/10.1016/j.msec.2008.10.037>.
- [10] R. Shi, Y. Tian, L. Wang, *Bioinspired Fibers with Controlled Wettability: From Spinning to Application*, ACS Nano 15 (5) (2021) 7907–7930. <https://doi.org/10.1021/acsnano.0c08898>.
- [11] A. Raman, J. S. Jayan, B. Deeraj, A. Saritha, K. Joseph, *Electro-*

- spun Nanofibers as Effective Superhydrophobic Surfaces: A Brief review, *Surfaces and Interfaces* 24 (2021) 101140. <https://doi.org/10.1016/j.surfin.2021.101140>.
- [12] J. Chen, Z.-X. Low, S. Feng, Z. Zhong, W. Xing, H. Wang, Nanoarchitectonics for Electrospun Membranes with Asymmetric Wettability, *ACS Applied Materials & Interfaces* 13 (51) (2021) 60763–60788. <https://doi.org/10.1021/acsami.1c16047>.
- [13] S. S. Dani, B. Sundaray, S. K. Nayak, S. Mohanty, Electrospun PVDF and composite nanofiber: Current status and future prescription towards hybrid Piezoelectric nanogenerators, *Materials Today Communications* 38 (2024) 107661. <https://doi.org/10.1016/j.mtcomm.2023.107661>.
- [14] F. Mokhtari, A. Samadi, A. O. Rashed, X. Li, J. M. Razal, L. Kong, R. J. Varley, S. Zhao, Recent progress in electrospun polyvinylidene fluoride (PVDF)-based nanofibers for sustainable energy and environmental applications, *Progress in Materials Science* 148 (2025) 101376. <https://doi.org/10.1016/j.pmatsci.2024.101376>.
- [15] R. Abdulhussain, A. Adebisi, B. R. Conway, K. Asare-Addo, Electrospun nanofibers: Exploring process parameters, polymer selection, and recent applications in pharmaceuticals and drug delivery, *Journal of Drug Delivery Science and Technology* 90 (2023) 105156. <https://doi.org/10.1016/j.jddst.2023.105156>.
- [16] S. Kailasa, M. S. B. Reddy, M. R. Maurya, B. G. Rani, K. V. Rao, K. K. Sadasivuni, Electrospun Nanofibers: Materials, Synthesis Parameters, and Their Role in Sensing Applications, *Macromolecular Materials and Engineering* 306 (11) (2021) 2100410. <https://doi.org/10.1002/mame.202100410>.
- [17] K. Karpagavel, K. Sundaramahalingam, A. Manikandan, D. Vanitha, A. Manohar, E. R. Nagarajan, N. Nallamuthu, Electrical Properties of Lithium-Ion Conducting Poly (Vinylidene Fluoride-Co-Hexafluoropropylene) (PVDF-HFP)/Polyvinylpyrrolidone (PVP) Solid Polymer Electrolyte, *Journal of Electronic Materials* 50 (8) (2021) 4415–4425. <https://doi.org/10.1007/s11664-021-08967-9>.
- [18] V. Eyupoglu, A. Unal, E. Polat, B. Eren, R. Ali Kumbasar, An efficient cobalt separation using PVDF-co-HFP based ultrafiltration polymer inclusion membrane by room temperature ionic liquids, *Separation and Purification Technology* 303 (2022) 122201. <https://doi.org/10.1016/j.seppur.2022.122201>.
- [19] X. Xing, X. Zhang, M. A. S. Tasin, X. Liang, H. Zhou, H. Niu, Interlaced Amphiphobic Nanofibers for Smart Waterproof and Breathable Membranes with Instant Waterproofness Monitoring Ability, *ACS Applied Polymer Materials* 6 (12) (2024) 7301–7310. <https://doi.org/10.1021/acsapm.4c01305>.
- [20] Y. Yang, Z. Guo, Y. Li, Y. Qing, P. Dansawad, H. Wu, J. Liang, W. Li, Electrospun rough PVDF nanofibrous membranes via introducing fluorinated SiO₂ for efficient oil-water emulsions coalescence separation, *Colloids and Surfaces A: Physicochemical and Engineering Aspects* 650 (2022) 129646. <https://doi.org/10.1016/j.colsurfa.2022.129646>.
- [21] Y. Xiao, F. Xie, H. Luo, R. Tang, J. Hou, Electrospinning SA@PVDF-HFP Core-Shell Nanofibers Based on a Visual Light Transmission Response to Alcohol for Intelligent Packaging, *ACS Applied Materials & Interfaces* 14 (6) (2022) 8437–8447. <https://doi.org/10.1021/acsami.1c23055>.
- [22] T. U. Rashid, R. E. Gorga, W. E. Krause, Mechanical Properties of Electrospun Fibers—A Critical Review, *Advanced Engineering Materials* 23 (9) (2021) 2100153. <https://doi.org/10.1002/adem.202100153>.
- [23] F. Russo, R. Castro-Muñoz, S. Santoro, F. Galiano, A. Figoli, A review on electrospun membranes for potential air filtration application, *Journal of Environmental Chemical Engineering* 10 (5) (2022) 108452. <https://doi.org/10.1016/j.jece.2022.108452>.
- [24] M. Heinz, P. Stephan, T. Gambaryan-Roisman, Influence of nanofiber coating thickness and drop volume on spreading, imbibition, and evaporation, *Colloids and Surfaces A: Physicochemical and Engineering Aspects* 631 (2021) 127450. <https://doi.org/10.1016/j.colsurfa.2021.127450>.
- [25] A. Rawal, S. Shukla, S. Sharma, D. Singh, Y.-M. Lin, J. Hao, G. C. Rutledge, L. Vásárhelyi, G. Kozma, A. Kukovec, L. Janovák, Metastable wetting model of electrospun mats with wrinkled fibers, *Applied Surface Science* 551 (2021) 149147. <https://doi.org/10.1016/j.apsusc.2021.149147>.
- [26] J. E. Domínguez, A. Kasiri, J. González-Benito, Wettability behavior of solution blow spun polysulfone by controlling morphology, *Journal of Applied Polymer Science* 138 (15) (2021) 50200. <https://doi.org/10.1002/app.50200>.